Journal of
Water & Climate Change

IWA PUBLISHING

Journal of Water and Climate Change Vol 13 No 2, 1007 doi: 10.2166/wcc.2021.436

Simulation-optimization framework in urban flood management for historic and climate change scenarios

R. Madhuri, Y. S. L. Sarath Raja and K. Srinivasa Raju*

Department of Civil Engineering, BITS Pilani, Hyderabad Campus, Hyderabad 500 078, India
*Corresponding author. E-mail: ksraju@hyderabad.bits-pilani.ac.in

ABSTRACT

A simulation-optimization framework is established by integrating Hydrologic Engineering Center Hydraulic Modeling System (HEC-HMS) for computation of runoff, siting tool EPA System for Urban Storm-water Treatment and Analysis INtegration (EPA-SUSTAIN) for placement of Best Management Practices (BMPs), and Binary Linear Integer Programming (BLIP) for runoff reduction. The framework is applied to an urban catchment, namely Greater Hyderabad Municipal Corporation (GHMC). The rainfall-runoff analysis was conducted for extreme rainfalls for historic (2016) and future events in 2050 and 2064 under Representative Concentration Pathways (RCPs) 6.0 and 8.5. The simulation-optimization approach in the historic scenario yielded 495,607 BMPs occupying 76.99 km^2 resulting in runoff reduction of 21.54 mm (198.76–177.22 mm). Achieved runoff reduction is 38.72 (428.35–389.63 mm) and 55.03 (602.65–547.62 mm), respectively, for RCPs 6.0 and 8.5, which could meet the water demands of GHMC for 10.33 and 11.53 days. Impacts of 10 different BMP configurations of varying costs (10–70%) and pollutant load reductions (0–3%) on runoff reduction are accomplished as part of sensitivity analysis.

Key words: BLIP, BMP, GHMC, HEC-HMS, Siting tool

HIGHLIGHTS

- Simulation-optimization framework for best management practices to an urban catchment of GHMC for historic and two RCP-based extreme event rainfall scenarios.
- Studying the applicability of EPA-SUSTAIN BMP siting tool, screening procedure, and BLIP for placement of BMPs for historic rainfall event and two RCP-based extreme event rainfall scenarios.
- Flood preparedness by implementing BMPs in an urbanized catchment.

INTRODUCTION

Rapid urbanization has a significant effect on urban floods. This situation has further deteriorated due to climate change, which results in an increment in the frequency of short-duration heavy intensity rainfall (Zhuang *et al.* 2019). Many studies proposed Best Management Practices (BMPs) for storm-water runoff quantity and quality control to mitigate urban floods (Lucas & Sample 2015; Esmail & Suleiman 2020). BMPs offer one of the best solutions for flood preparedness in an urban catchment (Li *et al.* 2019). With more rainfall intensity, the runoff volume captured by the BMPs increases (Lewellyn *et al.* 2016; Hou *et al.* 2020). The placement of BMPs can reduce flooding, pollutant load, economic loss, human loss, and health hazards (Boguniewicz-Zabłocka & Capodaglio 2020). It also improves ecological conditions while providing opportunities for water conservation, infiltration, and potable water saving (Antolini *et al.* 2020; Sarma & Rajkhowa 2021). BMPs include rain gardens, bioretention, rain barrels, vegetated rooftops, and permeable pavements (Braune & Wood 1999; Gülbaz & Kazezyilmaz-Alhan 2015). However, determining the optimal location, placement, and selection of cost-effective BMPs to obtain maximum runoff reduction is a challenge in the case of an urban watershed with distributed rainfall (Qin *et al.* 2013). These necessitate efficient modeling approaches (Adham *et al.* 2016) that assess BMP effectiveness (Yao *et al.* 2015). Relevant literature related to runoff-based study of BMPs, siting tool, screening, and simulation-optimization are as follows:

Runoff-based study of BMPs

Many studies have used runoff models, namely the Storm Water Management Model (SWMM) and Hydrologic Engineering Center Hydraulic Modeling System (HEC-HMS) for estimation of runoff (Zoppou 2001). Oleyiblo & Li (2010) utilized HEC-HMS and HEC-GeoHMS for Misai and Wan'an catchments in China. They confirmed the model's appropriateness, capacity, and reasonableness for flood forecasting in catchments. Ramly & Tahir (2016) used HEC-GeoHMS and HEC-HMS to simulate flood at the upper Klang–Ampang River Basin, Malaysia, and processed the Digital Elevation Model (DEM) in the ArcGIS 10.2 environment. The simulated and observed discharges were 308.7 and 298.8 m^3/s, respectively. Sarminingsih *et al.* (2019) analyzed the rainfall-runoff relationship for Garang watershed, Semarang, Indonesia, using HEC-HMS. They found that HEC-HMS was suitable enough to model the rainfall-runoff process. Karunanidhi *et al.* (2020) performed rainfall-runoff analysis for the Lower Bhavani river, India, and found that the annual runoff varied from 102.04 to 463.02 mm. The basin's average surface runoff volume would be 81×10^6 m^3, respectively, according to the Soil Conservation Service-Curve Number (SCS-CN) model. The number of researchers applied HEC-HMS for India (Islam *et al.* 2014; Ramachandran *et al.* 2019) and elsewhere (Ramly & Tahir 2016; Sarminingsih *et al.* 2019). However, very few investigated the impact of BMPs for runoff reduction in association with HEC-HMS. Hence, a study on the applicability of BMPs and their location identification for urban runoff computation is of utmost significance. Location of BMPs can be facilitated with a siting tool: EPA System for Urban Storm-water Treatment and Analysis INtegration (EPA-SUSTAIN 2014).

A limited number of researchers used SUSTAIN, which has SWMM as an inbuilt runoff estimation model, to locate BMPs. Kurkalova (2014) discussed BMP selection and placement aspects and concluded that the cost-effectiveness of BMPs and placement played a significant role in financial strategy. Similar views are echoed on the placement of BMPs by Sun *et al.* (2016).

Lee *et al.* (2012) used SUSTAIN for placing porous pavement and bioretention for 23 sub-watersheds in Kansas City, USA. They concluded that 2.2 and 1.6% of an entire watershed could be changed to bioretention and porous pavement. Jia *et al.* (2015) implemented bioretention, rain barrel, porous pavement, grassed swale, and green roof using SUSTAIN for cost-effective placement at a college campus in Foshan, China. Total peak flow, runoff volume, and pollutant loads decreased by 13.8, 14.5, and 17–21%, respectively. Warganda & Sutjiningsih (2017) studied BMPs in an urban watershed at Universitas Indonesia Campus, Indonesia. They assessed the performance of ten types of BMPs and justified the applicability of SUSTAIN for placement of BMPs at strategic locations. You *et al.* (2019) implemented Low Impact Development (LID)/BMPs in a residential community of China using SUSTAIN, and achieved a runoff reduction of 38.8% with a cost of $ 1.7 million.

Beck (2014) employed SUSTAIN to quantify BMP implementation impacts in Ballona Creek, Dominguez Channel, and Los Angeles River watersheds. Seven BMP types were optimized using Non-dominated Sorting Genetic Algorithm-II (NSGA-II) for the cost-effectiveness curve. Results indicated that dry weather total daily load (TMDL) could reduce by 80–99%, and 10–50% in wet weather TMDL. The reduction of 20–50% in peak runoff is noticed along with groundwater recharge of 12,000–30,000 ac-ft per year.

Shishegar *et al.* (2018) expressed that mathematical modeling is an effective way of optimizing the performance of BMPs and suggested categorization of different techniques such as Linear Programming (LP) and Non-Linear Programming (NLP). Loáiciga *et al.* (2015) applied Binary Linear Integer Programming (BLIP) for selecting two types of BMPs for a case study of Boulevard, USA. They found BLIP to be advantageous for deciding whether to place or not to place the specified BMPs developed with standardized designs. Sadeghi *et al.* (2018) used the Mixed Integer Linear Programming (MILP) model with La Recarga runoff model for placing BMPs in Los Angeles city, CA. Wu *et al.* (2020) studied optimal combination of LIDs for Gongming, Shenzhen, South China.

Increments in urban floods are anticipated due to climate change in the years to come. Therefore, similar studies to that of the historic scenario to gauge the impact of placing BMPs on urban flood mitigation need to be conducted. In this regard, the following section discusses the literature review related to impacts of climate change.

Climate change aspects

Coupled Model Intercomparison Project 5 (CMIP5) initiated the mechanism of Global Climate Models (GCMs), and Representative Concentration Pathways (RCPs) to assess future rainfall in climate change situations (Taylor *et al.* 2012). Khaing (2015) studied the impact of climate change (ICC) on hydropower generation and streamflow in the Myitnge river basin, Republic of the Union of Myanmar. He applied HEC-HMS to study the changes in hydrological regimes of the future, and projected a decrease in long-term average annual discharge using 2 GCMs. There was a decreasing discharge trend in RCP 8.5 of GFDL-CM3 with a range of 18–23% and 13–25% in Upper Yeywa and Yeywa, respectively. Rukundo &

Doğan (2016) studied the occurrence of floods for Kigali city, Rwanda, Africa. They used HadCM3 with A2 and B2 scenarios. An increase in rainfall is expected in June 2020 (30.2%), May 2070 (27%), and November 2070 (23.6%) for HadCM3-A2. Das *et al.* (2018) focused on scenario uncertainty and modeling, using the possibility theory and reliability ensemble averaging for projecting stream flows over the Wainganga river basin, India. They found that MPI-ESM-LR in the RCP 8.5 scenario has the highest possible value compared to RCP 4.5. A similar increasing trend is found for HadCM3-B2. Effects of climate change on urban floods in northern China are studied by Zhou *et al.* (2018). The flood volume increase is noted under RCP 8.5. Zhou *et al.* (2019) found that changes caused by urbanization on runoff were significantly higher than climate change. Nilawar & Waikar (2019) quantified climate change impacts on streamflow and sediment concentration in India's Purna river basin, under RCPs 4.5 and 8.5 for four future periods. An increment in both was found as compared to the baseline condition. Ramachandran *et al.* (2019) performed integrated flood modeling with HEC-HMS and HEC-RAS over Adyar sub-basin, India using data of 5 GCMs and RCP 4.5. There is an increase of 34.3–91.9% in the peak discharge and 12.6–26.4% in the flooded area compared to the present climate.

Kuntiyawichai *et al.* (2020) used HEC-HMS to generate hydrographs based on three GCMs, RCPs 4.5 and 8.5 for the lower Nam Phong River Basin, Thailand. Flood damage under RCP 4.5 was more significant than that of the baseline. Avashia & Garg (2020) found that the number of flood events in 42 Indian cities is considerably lower in RCP 2.6 than RCPs 4.5 and 8.5. An increase in mean annual precipitation under RCP 8.5 is noticed. Lee *et al.* (2021) evaluated hydrological risks of *n*-year floods in Korea. An increase in hydrologic flood risk was observed as compared to the present level. Lompi *et al.* (2021) simulated the rainfall-runoff process and the associated flood risks of future scenarios for a case study of Pamplona. Design peak discharge is higher in RCP 8.5 than in RCP 4.5. Mandal *et al.* (2021) employed SWAT for the Subarnerekha river basin for computing river discharges and other hydrological fluxes. An increase in rainfall for all RCPs is reported. Javadinejad *et al.* (2021) studied climate change impact on storm-water and the probability of maximum flood for the Zayandeh rud river basin, Iran. Maximum probable precipitation in the basin for RCPs 2.6, 4.5, and 8.5 can change by +5, −5, and −10% for the period of 2006–2040 as compared to that of 1970–2005.

As inferred from the literature review, limited studies have discussed various aspects of BMP placement, runoff estimation, and optimization procedures for historic and climate change scenarios (Ramachandran *et al.* 2019; Kuntiyawichai *et al.* 2020). Accordingly, research gaps identified were as follows:

1. Limited studies on the analysis of BMP siting and placement for historic and climate change scenarios.
2. No study is reported on the Ratio of Runoff Reduction to Cost (RRRC) as a screening process before optimizing the location of BMPs.
3. Limited studies are reported on utilizing BLIP for placement or non-placement of BMPs.
4. Limited studies are noticed on considering existing policies of government and infrastructure creation.
5. No extensive studies are reported for Indian conditions.

Accordingly, a simulation-optimization approach was proposed including runoff simulation, BMP siting, and screening based on RRRC, followed by optimal placement of BMPs using BLIP. Hence, the objectives both in historic and climate change scenarios after considering research gaps are as follows:

1. To compute basin-wise runoff using HEC-HMS.
2. To site locations of potential BMPs using EPA-SUSTAIN BMP.
3. To screen multiple BMPs through a two-phase screening process, i.e., satellite imagery (primary screening) and then based on RRRC (secondary screening).
4. To employ BLIP for achieving an optimal combination of BMPs for maximum runoff reduction in terms of placement or non-placement of BMPs.

METHODOLOGY

The developed methodology (refer to Figure 1) was applied to Greater Hyderabad Municipal Corporation (GHMC). The workflow is as follows: EPA-SUSTAIN BMP siting tool has been used to determine the potential location of BMPs. Here, BMP siting and screening procedures were performed in sequence. Runoff values have been simulated using HEC-HMS independently. Later, BLIP optimization was performed for optimal placement of BMPs by using simulated runoffs and calculated pollutant loads. In addition, impacts of BMP placement on runoff for various combinations of budget availability (BA) and

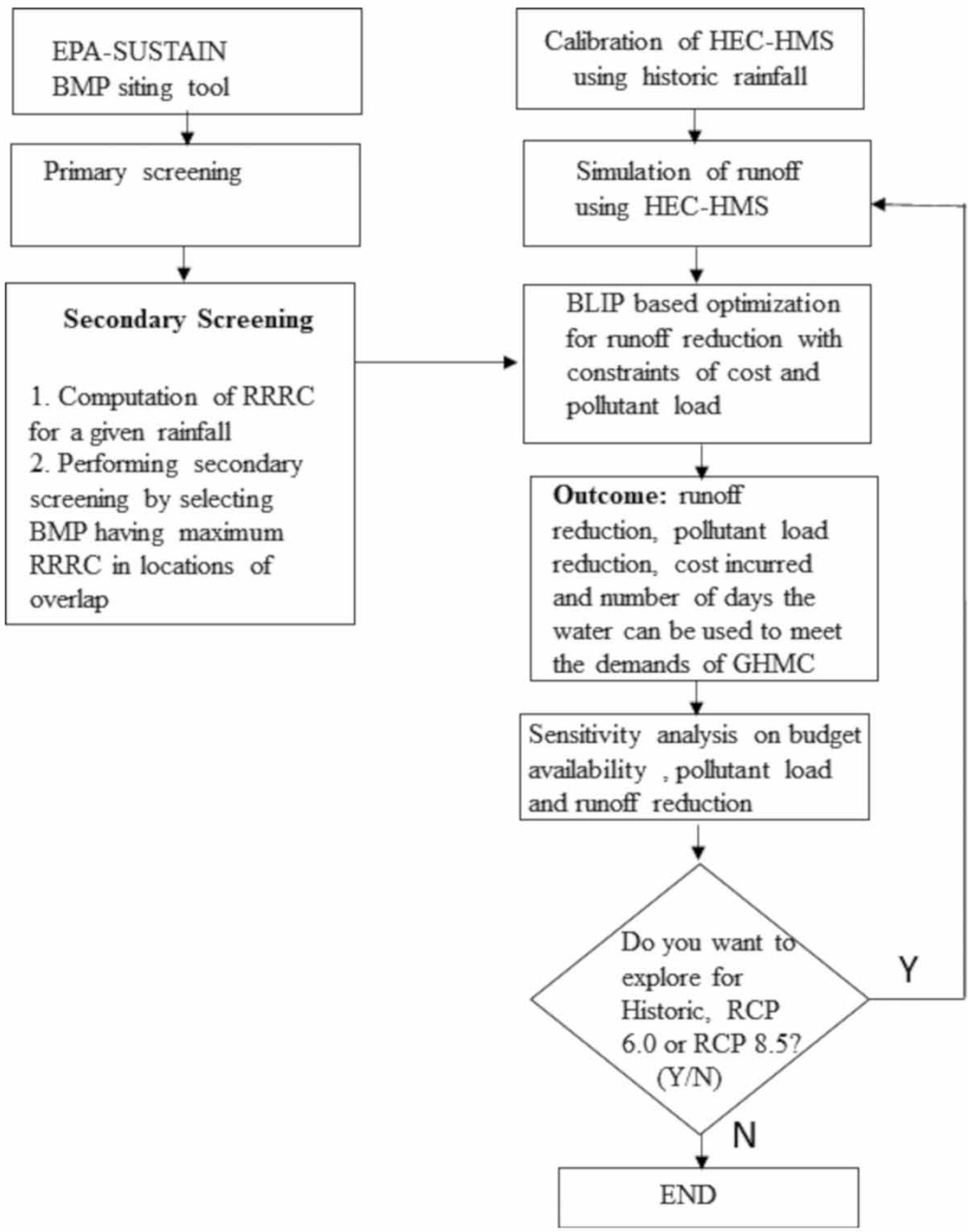

Figure 1 | Flowchart of the framework.

pollutant load are studied. This process is repeated for historic RCPs 6.0 and 8.5. The developed mechanism ensures efficient utilization of available open spaces in an urbanized catchment and rooftops for reducing the severity of floods and damage caused due to excess runoff. A case study, data collection and processing details, which are part of the methodology, are presented next.

Case study

GHMC has an area of 625 km^2 that falls in the catchment of the Musi river (11,000 km^2). It is divided into 16 zones based on a storm-water network (Figure 2) and gets an annual average rainfall of 840 mm. Due to its undulating topography in some

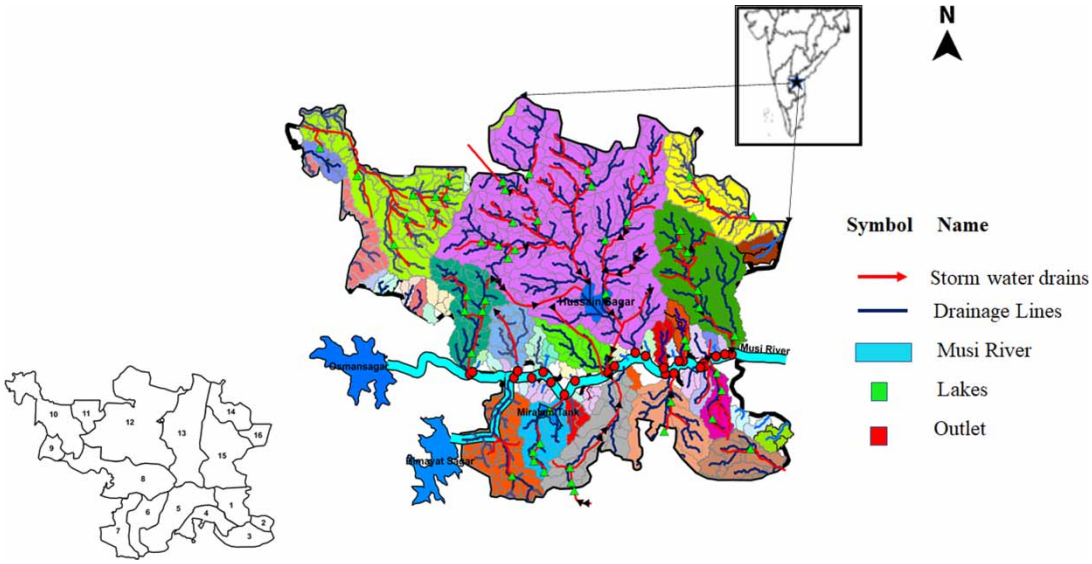

Figure 2 | Watershed area of GHMC showing natural drainage, lakes, and storm-water drainage with multiple outlets (modified and adapted from GHMC).

areas and increase in imperviousness, rainwater tends to gather in the low-lying regions resulting in loss of property (Vemula *et al.* 2019). Hence, there is a need for runoff reduction. BMPs can facilitate the same in the available open space of 125 km^2, approximately 20% of the urban catchment.

Data collection and processing

Salient data collected and processed are rainfall, runoff, land use land cover (LULC), population, and reduction efficiencies. Brief but relevant information is as follows:

Historic rainfall data is collected from GHMC and the Directorate of Economics and Statistics (DES) for 2016. The temporal distribution was assumed to be uniform over 24 h. In the climate change scenario, the future extreme rainfall events analyzed are from 2006–2100. They are based on GCM, Geophysical Fluid Dynamics Laboratory Coupled Physical Model (GFDL-CM3), and the non-linear regression-based statistical downscaling technique was used to downscale the RCP scenarios to the catchment scale (Vemula *et al.* 2019; Swathi 2020). Event-based extreme events are considered as follows:

- 440.35 mm (0.30, 7.21, 79.42, 117.61, 181.69, 35.39, 3.40, 2.33, 3.30, 2.71, 1.26, 0.88, 1.33, 1.99, 0.78, 0.57, and 0.18 mm, mid-century extreme event, 2050) for RCP 6.0.
- 624.2 mm (0.21, 0.10, 1.29, 1.39, 0.83, 0.89, 2.82, 3.93, 5.27, 10.55, 17.78, 17.42, 15.70, 33.04, 48.59, 324.14, 135.86, 3.45, and 0.94 mm, mid-century extreme event, 2064) for RCP 8.5.

More details about the event-based approach are available in the Supplementary material (refer to Section S1). In the present study, only RCPs 6.0 and 8.5 were chosen for demonstration (Vemula *et al.* 2019; Swathi 2020). However, detailed results related to the remaining two RCPs, 2.6 and 4.5, are available from the corresponding author on request.

Runoff data at Hussain Sagar corresponding to rainfall for September 1–19, 2016 was obtained from Hussain Sagar Lake Development Authority (HSLDA 2016). This runoff data was used for calibration as discussed in the calibration and runoff estimation section. The input data used is Advanced Space-borne Thermal Emission and Reflection Radiometer (ASTER)-based digital elevation model (DEM) of spatial resolution 30 m × 30 m (USGS 2016). Details of storm-water drainage network, soil data, water quality data of Hussain Sagar Lake, and guidelines for placing rainwater harvesting structures are available from the corresponding author on request. Percentage impervious land use was based on the supervised classification for 1995, 2006, and 2016. Imperviousness for 1991, 2001, and 2015 was obtained from Sannigrahi *et al.* (2018) and Nayan *et al.* (2020).

LULC data has been acquired from the open street maps (Open Street Maps 2016) of spatial resolution of 20 m. In addition, some of the building data were downloaded as shapefiles having 2.62 m multi-spectral spatial resolution (Google Earth 2016). LULC and imperviousness percentage of the year 2031 was prepared from the available Master plan of Hyderabad

Metropolitan Development Authority (HMDA 2019). Curve fitting is used to represent the available data by assigning a best-fit curve. The sigmoidal curve was found to be the best practical fit (with R^2 value of 0.9567) as it was adhering to the constraint of imperviousness percentage not exceeding 100%. Land imperviousness and CNs for future periods corresponding to RCPs 6.0 and 8.5 were extrapolated using the sigmoidal curve. Imperviousness is expected to increase to 84.85% by 2050 and 87.04% by 2064. Corresponding CNs were 88 and 89. The assessment of population for various time zones is needed. The polynomial fit was identified due to its higher R^2 value. The forecasted population for 2050 and 2064 was 1.902×10^7 and 2.420×10^7, respectively.

Table 1 presents depth, runoff, and pollutant load reduction efficiencies for different BMPs recommended for GHMC (Rao & Surinaidu (2012) for bioretention, Battiata *et al.* (2010) for vegetated filter strip, and HMWSSB (2012) for the remaining BMPs). Pollutant load reduction efficiency of each type of BMP varies from 0 to 75%, while runoff reduction efficiency varies from 10 to 80%. In addition, runoff reduction efficiencies for each BMP may not vary significantly across GHMC as the catchment is highly urbanized with predominantly sandy loamy soil (Rangari *et al.* 2021). Here, infiltration basin, infiltration trench, and rain barrel are termed as rooftop BMPs, whereas the remaining are non-rooftop BMPs (refer to Table 1).

Information about cost/m^3 was provided by HMWSSB (2018) for both rooftop and non-rooftop BMPs which are as follows:

1. Rooftop BMPs: Rs. 4,000 (Rs. 3,500 for placement and Rs. 500 for silt traps, gutters, or downspouts used for transporting the collected rainwater, leaf screens, first-flush diverters, and roof washers).
2. Non-rooftop BMPs: Rs. 3,850 (Rs. 3,500 for placement and Rs.350 for silt trap).

BMPs with specific dimensions and efficiencies were placed for historic scenario and will be assumed to be same for future scenarios by providing regular maintenance. Accordingly, 10% of construction and placement cost were considered, which is prevailing at present as the operation and maintenance (O & M) costs in the budget. O & M is assumed to be constant in the modeling framework and may vary according to change in the budget as communicated by HMWSSB authorities.

This increment in the budget was handled using a simple interest method (Equation (1)), where the increment in cost is treated as the O & M% for extended life (Pournara 2013).

$$\text{Total Cost} = \text{Construction and Placement Cost} \times \left(1 + n \times \frac{\text{O \& M\%}}{100\%}\right) \quad (1)$$

where construction and placement cost is the cost of constructing and installing the BMPs, O & M% is the additional % of construction and placement cost incurred as maintenance cost, and n is the number of years of maintenance. Total cost is the final cost incurred throughout the life of BMP. It will enable us to maintain the efficiency and life of BMPs in the future.

METHODS

Details of HEC-GeoHMS/HEC-HMS project setup, EPA-SUSTAIN siting tool, screening procedures, and BLIP are as follows:

HEC-GeoHMS is an extension of HEC-HMS, which works on the Geographical Information System (GIS) platform. It helps users to visualize and analyze spatial data, delineate sub-basins and streams that provide inputs to HEC-HMS. All the GIS data layers representing sub-catchments, conduits, junctions, and outfall were imported to HEC-HMS to develop the model structure for runoff calculation. HEC-HMS consists of five modules as follows:

- In the basin module, each sub-basin is provided with a specific CN and types of losses.

Table 1 | BMPs and their reduction efficiencies and depth (Battiata *et al.* 2010; HMWSSB 2012; Rao & Surinaidu 2012)

BMP reduction efficiency (%)	Infiltration basin	Infiltration trench	Rain barrel	Vegetated filter strip	Porous pavement	Grassed swales	Constructed wetland	Wet pond	Bioretention	Sand filter surface
Runoff (P_i) (1)	70	70	70	57	75	60	10	10	80	50
Pollutant load (l_i) (2)	15	25	0	50	25	35	75	75	60	45
Depth (m)	3	3	3	0.5	0.6	0.5	1	1	3	1

- In the meteorological module, each sub-basin is assigned with rain gauge information. The rain gauges were set to various catchments based on the Thiessen polygon approach. Rainfall data were transferred to respective sub-catchments based on a specified hyetograph method.
- The start date and end date of rainfall data were given as temporal input for each sub-basin in the control specifications module.
- Time-series data were given as rainfall input based on rain gauge information in the time-series module.
- Storage discharge functions were mentioned as necessary reservoir conditions to calculate runoff in the paired data manager module.

The runoff computation was dependent on CN employed for calibration of each sub-basin, and accordingly, final runoff could be obtained at the outlet. The shapefiles created in HEC-GeoHMS are supported as background maps in HEC-HMS and flow connectivity operations. The peak discharges, runoff volume, and runoff depth for each sub-catchment, junction, and outlet were calculated. This information was required for calibrating the model.

EPA-SUSTAIN (2014) BMP siting tool suggests multiple feasible BMPs for a given location based on its topographical features employing a suitability criteria matrix. Input/criteria include slope, drainage area, hydrologic soil group, imperviousness, depth of water table, building buffer, road and stream buffer, land ownership, and land use suitability (Cheng *et al.* 2009). The siting tool uses a concept of buffer, where a strip of land around or from the feature (i.e., roads, railways, and streams) is available for placement of BMPs. In this tool, volume-dependent BMPs (bioretention, rain barrel, constructed wetland, grassed swales, infiltration basin, infiltration trench, sand filter surface, and vegetated filter strip) and area-dependent (porous pavement) BMPs were considered.

However, we can place only one BMP in a given location. This constraint is due to land use, location specifications, materials used, and the constitution of BMPs. In addition, the efficiencies of BMPs are not the same (Table 1). It prevents the use of two BMPs of different categories over the same area. For this purpose, a two-stage screening procedure consisting of primary screening and secondary screening was developed. Primary screening was established on background satellite imagery used for ground-truthing. Here, ground-truthing implies interpretation of remotely sensed satellite images in the form of aerial photographs (raster images or vectorial map representation in GIS), making decisions on on-site supervision and compatibility of BMPs with surface characteristics. This ensures that incompatible BMPs in terms of land use are not considered. Accordingly, more suitable BMPs were prioritized over other overlapping BMPs. Suitability criteria applied for primary screening is that a vegetated filter strip is preferred on the circumference of the lakes or water bodies. Similarly, sand filter surface, porous pavement beside roads or pavements, sand filter surface near buildings, grassed swales along the railway lines, bioretention in open areas, infiltration trench, infiltration basin, and rain barrel for rooftop harvesting. A secondary screening module filters BMPs located at the same place in such a way that one BMP per location is achieved. The secondary screening was based on the ratio of runoff reduction volume capability of each BMP to the cost of respective BMP.

Figure 3 displays a visualization of the effects of screening on overlapping BMPs at a given location. BMPs are first sited using the siting tool (Figure 3(a)) followed by a primary screening where BMPs are screened based on their suitability with their respective location(s) (Figure 3(b)). The primary screened BMPs then go through a secondary screening process where a decision is made based on RRRC for placement of cost-effective BMP (Figure 3(c)).

For secondary screening, the runoff reduction volume capability of each BMP was computed using Equation (2). The total cost of each BMP was calculated based on the unit cost (including material cost, labor cost, and digging cost), the cross-sectional area of each BMP, and the depth of BMP (Equation (3)).

$$\text{Runoff reduction volume capability of } i\text{th BMP}, \quad V_i = A_i R_i P_i \tag{2}$$

$$\text{Cost of } i\text{th BMP}, \quad C_i = C_{u,i} U_i \tag{3}$$

Accordingly, RRRC is V_i/C_i. Here, $i = 1, 2, \ldots, n$ are the number of BMPs; V_i is the runoff reduction volume capability of ith BMP (m^3); A_i is the cross-sectional area occupied by ith BMP (m^2); R_i is rainfall at a location where the ith BMP is placed (m); P_i is the runoff reduction efficiency of ith BMP (%) (row 1 of Table 1); C_i is the cost of ith BMP (Rupees); $C_{u,i}$ is the cost of ith BMP (m^3) (Rupees); u = '1' or '2' where '1' = Rooftop BMP and '2' = Non-rooftop BMP, and U_i is the volume occupied by ith BMP (m^3).

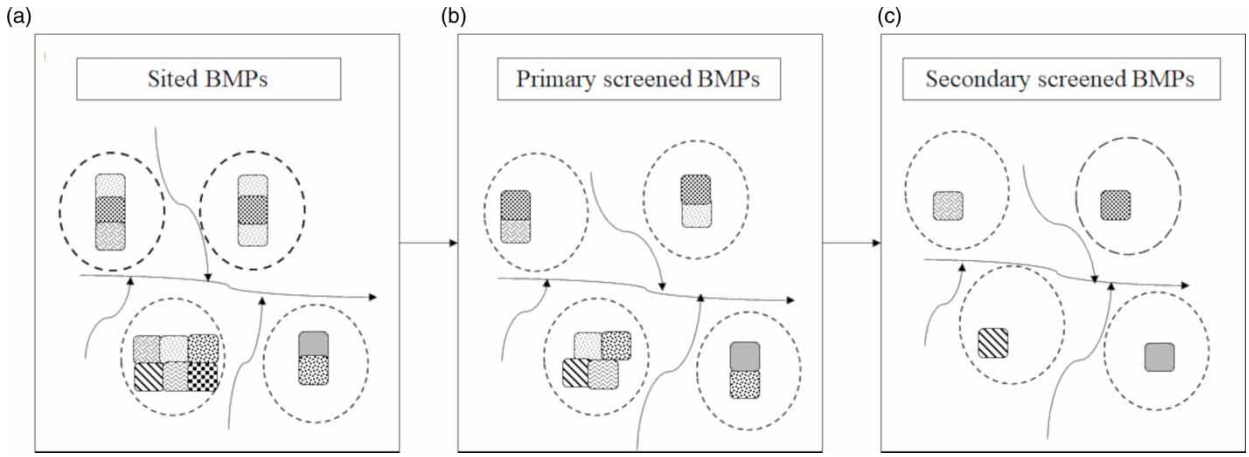

Figure 3 | Effect of screening on overlapping BMPs at a given location: (a) siting tool results, (b) primary screening results, and (c) secondary screening results.

Upon completion of the screening process, BLIP-based optimization was performed to ensure optimal placement of BMPs. It was assumed during modeling that (a) only one BMP can be placed in the available space, i.e., the placement of a BMP was assumed as 1, and non-placement was considered zero, (b) the depth of the BMP will not vary, and (c) the location of BMPs are fixed for both RCPs while harvesting rainwater.

The objective function chosen was the maximization of runoff reduction (Equation (4)) with constraints on cost (Equation (5)) as well as pollutant load reduction (Equation (6)):

$$\text{Maximize } Z = \sum_{i=1}^{n} V_i x_i \tag{4}$$

Subject to constraints,

$$\sum_{i=1}^{n} C_i\, x_i \;\le b \tag{5}$$

$$\sum_{i=1}^{n} L_i\, x_i \;\ge d \tag{6}$$

where L_i is the pollutant load reduction capability of ith BMP (in mg), i.e.,

$$R_{u,i}\, e_i l_i A_i \tag{7}$$

where x_i is the binary variable (value of 0 or 1); Z is the objective function representing runoff volume reduction; b is budget limitation; d is the pollutant load reduction target (mg); $R_{u,i}$ is the runoff at top of ith BMP of uth type (mm); e_i is the pollutant concentration over ith BMP (mg/l); and l_i is the pollutant load reduction efficiency of ith BMP in % (row 2 of Table 1). It should be noted that the values in Table 1 have no direct role in the modeling process (HEC-HMS or EPA-SUSTAIN BMP Siting Tool). However, they play a significant role in the screening and BLIP (Equations (2)–(6)) procedures, helping select the most appropriate BMPs.

The following section presents results and discussion related to historic and climate change scenarios where individual zones of GHMC are analyzed.

RESULTS AND DISCUSSION

Historic scenario

This section discusses computation of runoff, siting of BMPs, screening, and application of BLIP for the historic rainfall experienced by GHMC during September 20–28, 2016.

Calibration and runoff estimation

HEC-HMS was calibrated for the rainfall event of 176.9 mm (occurred during September 1–19, 2016) at zone 12 of GHMC. This event resulted in a flood depth of 0.5–3.9 m. It was found that areas in zone 5 are very highly vulnerable whereas areas of zones 1, 4, 10, and 12–15 are highly vulnerable (Surwase & Manjusree 2019; Vemula *et al.* 2019; Swathi *et al.* 2020). Calibration was performed for an observed runoff of 163 mm, and the resulting simulated value was 160.9 mm.

The spatial variation was taken into account by considering the runoff computation by the HEC-HMS model on a basin level using HEC-Geo HMS (USACE 2009). HEC-Geo HMS serves as a geospatial hydrologic modeling extension of HEC-HMS, which spatially generates all sub-basins based on catchment delineation of all streams. Significant inputs to HEC-GeoHMS were DEM and stream network. The stream network for the area was obtained from DEM by processing the Arc Hydro tool, which was a plugin in ArcGIS software. One hundred and twenty-eight sub-catchments were delineated based on stream order 3. Rainfall data from 12 rain gauge stations were available. The Thiessen polygon approach was employed due to its ability to spatially map the rainfall weights of each station with areal coverage (Ridwan *et al.* 2021). In addition, a sparse rain gauge network and less variability in rainfall are additional features that encouraged the use of the Thiessen polygon approach (Malik & Kumar 2020). The sub-watersheds were further grouped into ten different partitions for ease of evaluation. Based on this partition, ten junctions were identified where runoff could be calculated. Junctions were named based on the sub-catchments. Employed parameters, their ranges, obtained values, and remarks are presented in Table 2.

These calibrated values are obtained by comparing the simulated flows at the Hussain Sagar outlet for zone 12 with observed flows available from Hussain Sagar Lake Development Authority (HSLDA 2016). The calibration of HEC-HMS with observed flows resulted in an R^2 of 0.99 for zone 12 of GHMC. This enabled us to employ the same for future scenarios. Accordingly, all the 16 zones of GHMC were simulated for runoff for the extreme event rainfall, i.e., 215.9 mm for September 20–28, 2016. The summation of all these runoffs at the sub-basin outlets is the total runoff. The simulated runoff at the outlet for GHMC was determined to be 198.76 mm. Inference from the results was that zones 15, 12, 13, and 14 have the highest runoff values of 272.89, 252.75, 219.90, and 209.89 mm compared to other zones. Upon simulating the runoff values using HEC-HMS, we move ahead to discuss the results related to BMP siting.

BMP siting

BMPs were placed based on the feasibility constraints and GHMC guidelines. For example, buffer varies from 15 to 20 m for arterial roads. Here, buffer refers to the strip of land in the periphery of roads or streams, i.e., the maximum distance within

Table 2 | Employed parameters in HEC-HMS, ranges, obtained values, and remarks

S. No.	Methods	Parameters	Ranges	Calibrated values	Remarks, if any
1	Loss rate parameter	Curve number	71–89	85	It depends on land use and soil (sandy loam)
2		Impervious area (%)	60–85	73	Depends on land use
3		Initial abstraction (mm) I_a	0	0	For urban catchment $I_a = 0$
4	Runoff transform	Lag time	0.6 × (time of concentration T_c) minutes	60 min	T_c is calculated using Kirpich formula (varies for each basin, length, and slope)
5	Routing method constants	K (Travel time through the reach) (hours)	0–1	0.5	Depends on flow properties and knowledge of cross-section
6		x (Weighing factor between inflow and outflow influence)	0.0–0.5	0.2	0 refers to max attenuation; 0.5 refers to no attenuation

which BMP should be placed for roads and the minimum distance beyond BMP should be established for streams. Depth to water table from the ground affects the choice of specific BMPs. For example, drainage area $>1.01 \times 10^5$ m^2 favors constructed wetland or wet pond; road buffer >30.48 m favors all non-rooftop BMPs except bioretention, grassed swales, and vegetated filter strip. A high-water table (>0.61 and <1.22 m below ground level) will favor the choice of bioretention, grassed swales, porous pavement, sand filter surface, and vegetated filter strip over a constructed wetland or wet pond. As a note, only one type of rooftop BMP can be placed on any given building. However, competition existing among non-rooftop BMPs is mainly due to the terrain characteristics (EPA-SUSTAIN 2014). Table 3 (columns 2 and 3) presents results related to siting analysis as follows:

Out of 81.70 km^2, rooftop harvesting covers 75.04 km^2, more than non-rooftop BMPs, i.e., 6.66 km^2, thus significantly reducing runoff. Rooftop BMPs, namely infiltration basin, infiltration trench, and rain barrel, occupied 34.82, 38.29, and 1.93 km^2, respectively, totaling 75.04 km^2. The number of BMPs in this category was 88,415; 349,417; 54,440 totaling 492,272 out of 505,383 BMPs. The number and type of BMPs give an idea of the budget required for installation of BMPs. Since each BMP has specific efficiency, the number of BMPs will help to understand the amount of water thus saved. It also gives a quantitative idea of locations where BMPs can be placed. Reported results confirm that rooftop BMPs are more prominent than non-rooftop. It implies that the buildings can be used as a source of flood mitigation, and thereby proving itself an efficient BMP.

Porous pavement, sand filter surface, bioretention, grassed swales, vegetated filter strip, wet pond, and constructed wetland occupy respectively 0.58, 2.21, 2.16, 0.68, 0.85, 0.09, and 0.09 km^2, totaling 6.66 km^2. The number of bioretention BMPs was 2,882 out of total non-rooftop BMPs of 13,111, as bioretention has the highest RRRC among the non-roof top BMPs; and hence, it is prioritized over others. However, the sand filter surface with the highest number of BMPs of 3,661 is more economical and easily implementable. It was deduced from the results of zones 1 and 14 that a greater number of BMPs did not always necessarily mean occupying more area. Effects of screening were predominant in zone 8 implying that its terrain was the most compatible (satisfying the constraints mentioned) with the placement of different types of BMPs.

BMP screening modules

Primary screening (refer to columns 4 and 5 of Table 3*).* 498,908 BMPs were filtered, and the area covered by them was 78.72 km^2 (75.04 km^2 occupied by rooftop BMPs and 3.68 km^2 by non-rooftop BMPs). Reduction in non-rooftop BMPs area after primary screening is 2.98 km^2 as per siting analysis, and no visible effect on rooftop BMPs is found.

Table 3 | Types and area occupied by BMPs during siting, screening, and BLIP optimization procedures

	After BMP siting		After primary screening		After secondary screening			After BLIP	
Type of BMP (1)	Number of BMPs (2)	Area (km^2) (3)	Number of BMPs (4)	Area (km^2) (5)	Number of BMPs (6)	Area (km^2) (7)	Cost (Rs.) $\times 10^7$ (8)	Number of BMPs (9)	Area (km^2) (10)
Infiltration trench	349,417	38.29	349,417	38.29	349,417	38.29	918.96	349,240	38.28
Infiltration basin	88,415	34.82	88,415	34.82	88,415	34.82	835.78	88,363	34.65
Rain barrel	54,440	1.93	54,440	1.93	54,440	1.93	46.39	53,927	1.91
Sub-total Rooftop	492,272	75.04	492,272	75.04	492,272	75.05	1,801.13	491,530	74.84
Sand filter surface	3,661	2.21	2,597	1.74	1,944	1.40	537.46	1,588	1.14
Bioretention	2,882	2.16	692	0.52	622	0.39	74.31	600	0.38
Vegetated filter strip	2,774	0.85	1,492	0.58	1,215	0.44	84.32	1,107	0.38
Grassed swales	2,243	0.68	963	0.33	591	0.15	25.47	550	0.14
Porous pavement	1,169	0.58	623	0.34	196	0.08	18.48	194	0.08
Wet pond	191	0.09	158	0.09	110	0.07	26.95	37	0.03
Constructed wetland	191	0.09	111	0.07	6	0.00	0.39	1	0.00
Sub-Total Non-rooftop	13,111	6.66	6,636	3.68	4,684	2.52	767.36	4,077	2.15
Total	505,383	81.70	498,908	78.72	496,956	77.57	2,568.49	495,607	76.99

Secondary screening (refer to columns 6–8 of Table 3*)*. Analysis of data shows 496,956 BMPs (492,272 rooftop and 4,684 non-rooftop) covering an area of 77.57 km^2 (respectively 75.05 and 2.52 km^2). The reduction in BMPs from primary screening to secondary was 1,952, with a corresponding reduction in the area of 1.15 km^2. Zones 2 and 16 show no screening effect due to the absence of non-rooftop BMPs. The calculated cost of 496,956 BMPs was Rs. 25.68×10^9 (Rs. 18.01×10^9 for rooftop and Rs. 7.67×10^9 for non-rooftop). These are used further for estimating RRRC and for filtering BMPs for BLIP purposes. Post-screening locations of BMPs are presented in Figure 4. It is observed that the number of infiltration trenches is more, compared to other BMPs. Non-rooftop BMPs are fewer in number as the suitable open space available for BMP placement is comparatively fewer than the rooftop area. The total area of buildings in GHMC is around 84.91 km^2 which occupies 13.58% of the catchment area. In addition, zones 12 and 15 are presented in the Supplementary material (refer to Section S2). These two zones are presented due to their higher catchment areas of zone 12 (138 km^2) and zone 15 (67 km^2) and being more prone to flooding. However, other zones are not presented to minimize repetition.

As a note, EPA-SUSTAIN is used for determining the potential location of BMPs under the feasible constraints and screening procedures for removal of any overlap among BMPs. On the other hand, BLIP facilitates optimal placement or non-placement of BMPs.

Binary linear integer programming

BLIP is performed on the outputs of secondary screening adhering to its constraints of budget and pollutant load reduction. There is no minimum runoff reduction potential targeted in this study. This is because the runoff reduction capacity of BMPs varies with BA and pollutant reduction target. Accordingly, runoff reduction potential has been used only as an objective function in this paper and not as a constraint, thereby preventing the establishment of a condition on minimum runoff reduction. Higher budgets facilitate placement of more BMPs which, in turn, capture more surface runoff and vice-versa.

For this purpose, the total runoff was estimated by summing the individual runoffs at outlets of each zone, i.e., 142.21×10^6 m^3. Total pollutant load (TPL) was the product of total runoff value and BOD_3 of 14 mg/l (The Times of India 2018), resulting in 1,990.9 tonnes. Although reasonable estimates of water quality concerning BOD values were not available, as an attempt, this average value was introduced to the BMP placement mechanism by taking into consideration water quality as well. This process ensured a holistic approach toward evaluating the impacts of BMPs on runoff (water quantity and water quality). The perceived constraints were 100% BA and 3.38% TPL, i.e., Rs. 25.68×10^9 and 67.2 tonnes. With this

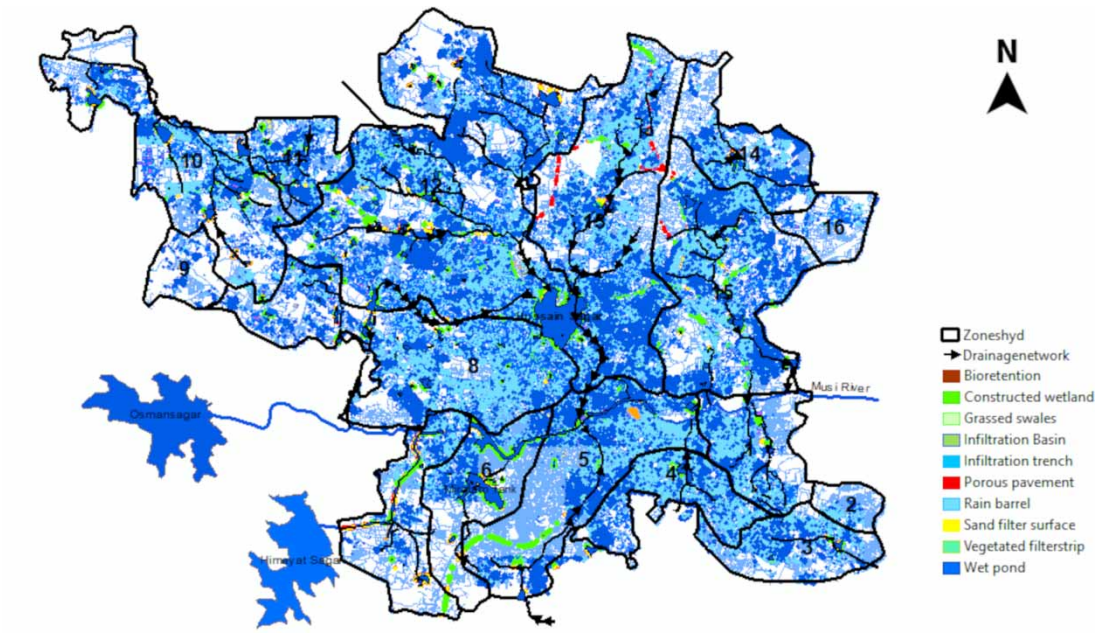

Figure 4 | Location of BMPs in GHMC.

information, BLIP was performed individually for an optimized placement combination of BMPs to reap benefits in maximizing runoff reduction.

BLIP resulted in 495,607 BMPs covering an area of 76.99 km^2. Infiltration basin and infiltration trench occupied 34.65 and 38.28 km^2, resulting in runoff reduction of 5.95 and 4.42%, respectively. Runoff at the outlet before placement of BMPs was 198.76 mm, whereas it is 177.22 mm after placement, showing a reduction of 21.54 mm. The budget utilized is Rs. 24.82×10^9, and the pollutant load reduction achieved was 67.38 tonnes. Runoff reduced was 15.41×10^6 m^3. It can be stored and utilized for urban catchment requirements. The population of GHMC was 8.99×10^6 in the year 2016 (GHMC 2011a, 2011b). Accordingly, the harvested water serves the need of the urban population for 11.43 days based on the requirement of 150 liters per capita per day (CPHEEO 1999). The analysis conducted here indicates that BMPs may be used for flood control and other conservation measures. The remaining possible combinations are discussed later in the sensitivity analysis section.

Climate change scenario

In an attempt, results related to two RCPs, 6.0 and 8.5, were presented here. Like the historic scenario, the simulation-optimization approach comprises HEC-HMS for simulating runoff, screening for filtering BMPs, and BLIP for optimization (refer to Figure 1). Calibrated parameters and projected population, LULC, and CN are used (refer to Data collection and processing section). The siting tool and screening procedure results will remain the same as the historic scenario, as these depend on the topographical constraints of land use and available space. Related results of RCPs 6.0 and 8.5 are as follows:

RCP 6.0

The equivalent runoff volume simulated was 33.29×10^7 m^3 for the year 2050 (RCP 6.0) for the rainfall of 440.35 mm using the HEC-HMS model. The runoff depth found was 428.35 mm. On the other hand, the pollutant load carried by the runoff was established on the simulated runoff volume and calculated as 4,660.21 tonnes. This was done by multiplying the simulated runoff volume of 33.29×10^7 m^3 with 14 mg/l (The Times of India 2018).

$$\text{Total pollutant carried by runoff} = 33.29 \times 10^7 \times 14 = 4,660.21 \text{ tonnes.}$$

Since the secondary screening results remain the same, the number of BMPs does not vary. But, since the BMPs need to be maintained to ensure their runoff and pollutant load reduction efficiencies, the budget increases due to these additional maintenance costs.

Therefore, the budget for placing all secondary screened BMPs and maintaining them will increase to Rs. 112.99×10^9 for RCP 6.0 (refer to Equation (1)). The achievable pollutant load reduction value was 42.13 tonnes. It is noted from BLIP results that the budget utilized is Rs. 108.50×10^9, and the final pollutant load reduction achieved is 136.54 tonnes. The number of BMPs utilized for this purpose is 492,149. Classifications of BMPs are infiltration trench (348,685), infiltration basin (88,177), rain barrel (51,137), sand filter surface (1,619), vegetated filter strip (1,129), bioretention (602), grassed swales (563), porous pavement (196), wet pond (40), and constructed wetlands (1). The resultant runoff experienced by the catchment is 389.64 mm, and the runoff reduced is 38.72 mm. Equivalent runoff volume reduced is 29.48×10^6 m^3. Water thus saved serves the GHMC for 10.33 days which is as follows:

$$\frac{\text{Runoff reduced } (m^3)}{\text{Per capita water consumption per day } (m^3) \times \text{Projected population}} = \frac{29.48 \times 10^6}{0.15 \times 1.902 \times 10^7} = 10.33 \text{ days}$$

RCP 8.5

Simulated runoff was 602.65 mm. The equivalent runoff volume was 46.78×10^7 m^3, and the pollutant load was 6,549.82 tonnes. Similarly, the achievable pollutant load reduction was 202.39 tonnes. The budget for placing all secondary screened BMPs and maintaining them was projected to increase to Rs. 148.95×10^9 for RCP 8.5. The budget utilized is Rs. 143.14×10^9, and the final pollutant load reduction achieved is 194.67 tonnes. The number of BMPs utilized for this purpose is 492,916. Classifications of BMPs are infiltration trench (349,228), infiltration basin (88,369), rain barrel (51,179), sand filter surface (1,623), vegetated filter strip (1,107), bioretention (603), grassed swales (570), porous pavement

(196), wet pond (40), and constructed wetlands (1). The resultant runoff is 547.63 mm, and the runoff reduced is 55.03 mm. Equivalent runoff volume reduced is 41.87×10^6 m^3. Water thus saved serves GHMC for 11.53 days.

Comparison of RCP 6.0 with RCP 8.5

In total, the simulated runoff was higher for RCP 8.5 than for RCP 6.0. The simulation-optimization mechanism resulted in a 9.04 and 9.13% runoff reduction by placing 492,149 BMPs and 492,916 BMPs, respectively, for RCP 6.0 and RCP 8.5 (difference of 767 BMPs concerning RCP 6.0). This difference in the runoff reduction percentages may be attributed to their duration, affecting the rainfall-runoff simulations in HEC-HMS. The runoff reduced under RCP 8.5 (46.78×10^7 m^3) is significantly higher than RCP 6.0 (33.29×10^7 m^3). However, the number of days this stored runoff can be used increases slightly (10.33 to 11.53 days). This is due to the increased (projected) population of 2.420×10^7 in 2064 (RCP 8.5) as compared to the projected population of 1.902×10^7 in 2050 (RCP 6.0), which demands more water consumption per day. Tables S1–S3 are presented in the Supplementary material showing the number and percentage of different types of BMPs for 100% BA for historic, RCPs 6.0, and 8.5 scenarios in respect of individual zones and GHMC. This provides enormous information about the number of rooftop and non-rooftop BMPs for these scenarios.

Sensitivity analysis

Impacts of different combinations of cost and pollutant load reductions on runoff volume reduction are studied. Related parameters were analyzed both for historic and climate change scenarios, which are as follows:

Historic scenario

Ten strategies were formulated for this purpose, namely *A* to *J*. *A* (10% BA, 0.34% TPL), *B* (20% BA, 0.68% TPL), *C* (30% BA, 1.02% TPL), *D* (40% BA, 1.36% TPL), *E* (50% BA, 1.7% TPL), *F* (60% BA, 2.05% TPL), *G* (70% BA, 2.39% TPL), *H* (80% BA, 2.73% TPL), *I* (90% BA, 3.07% TPL), *J* (95% BA, 3.24% TPL). Table 4 presents the related results.

Runoff reduction increased about seven times from 1.59 to 10.77% from strategies *A* to *J* (column 5 of Table 4). The number of BMPs increased from 99,278 (a total of 99,278 rooftop BMPs and 0 non-rooftop BMPs) to 495,165 (491,368 rooftop BMPs and 3,797 non-rooftop BMPs) (columns 8–10 of Table 4). Water demands of the entire population of GHMC are met for 1.68–11.36 days. 14.57×10^6 and 15.31×10^6 m^3 of the total runoff reduction can be achieved, and 472,974 out of 495,165 of the BMPs get placed with strategy *G* (70% BA and 2.39% TPL). This demonstrates the advantage of using BLIP to place BMPs where budgets can be efficiently utilized.

The rain barrel was in the order of minimum preference among rooftop BMP placements. It is due to the inability of a rain barrel for pollutant load reduction, which gives it the minimum weightage. This enlightens us by indicating that the more the pollutant reduction required in the constraints, the lower the number of rain barrels. The Supplementary material section

Table 4 | Binary linear integer programming results for historic scenario

Resources			Results							
Strategy (1)	Budget utilized (Rs.) $\times 10^9$ (2)	Final pollutant load reduction achieved (tonnes) (3)	Runoff reduced (m^3) $\times 10^6$ (4)	Runoff reduction (%) (5)	Runoff reduced (mm) (6)	Resultant runoff (mm) (7)	Number of rooftop BMPs (8)	Number of non-rooftop BMPs (9)	Total number of BMPs (10)	Number of days serving urban catchment (11)
A	2.55	16.11	2.27	1.59	3.17	195.59	99,278	0	99,278	1.68
B	5.12	25.92	4.51	3.17	6.31	192.45	169,361	59	169,420	3.35
C	7.68	34.09	6.72	4.73	9.4	189.36	239,510	165	239,675	4.99
D	10.21	41.99	8.9	6.26	12.44	186.32	297,341	229	297,570	6.60
E	12.78	49.61	11.07	7.79	15.48	183.28	371,721	290	372,011	8.21
F	15.33	56.65	13.02	9.15	18.19	180.57	423,695	451	424,146	9.66
G	17.81	62.1	14.57	10.25	20.37	178.39	471,906	1,068	472,974	10.81
H	20.23	64.71	15.02	10.56	21	177.76	484,298	2,540	486,838	11.14
I	22.66	66.29	15.26	10.73	21.33	177.43	491,052	3,350	494,402	11.32
J	23.81	66.86	15.31	10.77	21.4	177.36	491,368	3,797	495,165	11.36

mentions the detailed classification of BMPs from strategy A to J (refer to Section S3). Optimization results tend to follow the law of diminishing marginal utility from the moment the non-rooftop BMPs get placed. This is due to the impact of runoff reduction efficiency, pollutant reduction efficiency, depth, and a number of the BMPs, which play a significant role during optimization.

Effects of stabilization become evident from strategy '*F*' (60% BA and 2.05% TPL). This is because non-rooftop BMPs, which are relatively costly, come into existence. Even among the non-rooftop BMPs, the ones with lower cost are preferred. This is why about 94.5% of the total runoff reduction and 95.4% of the BMPs placement can be achieved with strategy G. Zones 12, 13, and 15 cover the significant proportion of the BMPs. The range of areas from *A* to *J* are 3.31–18.55 km^2 (zone 12), 1.96–12.86 km^2 (zone 13), and 1.93–11.8 km^2 (zone 15). This is due to their respective zone areas, which constrained the total open space available for BMP placement. Non-rooftop BMPs confirm the existence of stabilization. BMPs with a higher proportion of non-rooftop BMPs tend to show stabilization sooner than zones with a lesser ratio.

Climate change scenarios

Values of these constraints (columns 2 and 3 of Table 5) are chosen at random based on the maximum budget values and pollutant load reduction for the optimization process. Table 5 presents results for extreme future rainfall events under different BA and TPL constraints. From Table 5, it is observed (respectively, for RCPs 6.0 and 8.5 and 10–70% BA and different pollutant load targets) that:

It was found from Table 5 that in case for RCP 6.0, runoff reduced is 36.71, 22.28, and 5.71 mm for 70, 40, and 10% BA and 2.16,1.23, and 0.31% pollutant load reduction. The number of BMPs employed for this purpose are 470,049; 288,807; and 107,417. Water saved in this process serves the catchment for 9.8, 5.95, and 1.52 days, respectively. Similarly for RCP 8.5, runoff reduced is 52.16, 31.67, and 8.14 mm for 70, 40, and 10% BA and 2.19,1.25, and 0.31% pollutant load reduction. The number of BMPs employed for this purpose are 470,381; 291,652; and 109,403. Water saved in this process serves the catchment for 10.93, 6.64, and 1.71 days.

The number of BMPs placed for a given budget showed much less variation. Pollutant load reduction achieved can be found to increase from 29.01 to 125.97 tonnes and 43.26 to 153.79 tonnes (column 5 of Table 5). This reduction in pollutant load by placing BMPs helped preserve various lake bodies and reduce the load on Sewage Treatment Plants.

Urban density (the number of people inhabiting a given urbanized area) will increase in the coming years, increasing building, road, and railway line densities. It indicates that infiltration trenches, basins, rain barrels, porous pavements, and grassed swales will increase. On the other hand, open spaces and lakes may tend to reduce. Accordingly, vegetated filter strips, constructed wetland, wet pond, and bioretention may reduce. These urban sprawl results may affect the already placed BMPs of vegetated filter strips, constructed wetland, wet ponds, and bioretention, necessitating discarding them.

SUMMARY AND CONCLUSION

Hydrological model HEC-HMS, siting tool EPA-SUSTAIN, a two-stage screening procedure, and optimization model BLIP are coupled to develop a simulation-optimization framework that facilitates runoff reduction. Optimal utilization of all buildings and open spaces in an urban catchment that facilitates conservation of water following the guidelines and policies of the

Table 5 | BLIP results for 10, 40, and 70% budget availability, and different % TPL for two RCPs (budget available for RCP 6.0 and RCP 8.5 is Rs. 112.99×10^9 and 148.95×10^9 and TPL are 4 660.21 and 6 549.82 tonnes, respectively)

Resources			Results							
RCP scenarios (1)	Budget availability (BA) (2)	Pollutant load reduction target (3)	Budget utilized (Rs.) $\times 10^9$ (4)	Final pollutant load reduction achieved (tonnes) (5)	Runoff reduced (m^3) $\times 10^6$ (6)	Runoff reduction (%) (7)	Runoff reduced (mm) (8)	Resultant runoff (mm) (9)	Total number of BMPs (10)	Number of days serving urban catchment (11)
6.0	10%	0.31%	11.22	29.01	4.35	1.33	5.71	422.64	107,417	1.52
	40%	1.23%	44.97	81.25	16.97	5.2	22.28	406.07	288,807	5.95
	70%	2.16%	78.41	125.97	27.96	8.57	36.71	391.64	470,049	9.8
8.5	10%	0.31%	14.85	43.26	6.19	1.35	8.14	594.51	109,403	1.71
	40%	1.25%	59.45	116.95	24.10	5.26	31.67	570.98	291,652	6.64
	70%	2.19%	103.53	153.79	39.69	8.66	52.16	550.49	470,381	10.93

relevant agencies is also considered. Greater Hyderabad Municipal Corporation, India, is chosen as the case study for demonstration. Three extreme rainfall events considered are historic, RCP 6.0 and RCP 8.5.

We studied the impact of two situations. In the first situation, it is pre-BMP implementation (only HEC-HMS for computation of runoff). The second situation is post-BMP implementation (coupling of HEC-HMS, EPA-SUSTAIN, and BLIP). Runoff reduction is achieved because of the fundamental tendency of BMPs (having relatively high permeability) to allow water to permeate through it into the ground. The extent of permeability is determined by the runoff reduction efficiency, while pollutant trapping potential is a function of the pollutant reduction efficiency. The comparison of post- and pre-BMP implementation helped to understand the impact of BMPs on runoff.

In the historic extreme event, rainfall is 215.9 mm, and runoff is 198.76 mm (pre-placement of BMPs). However, after the placement of BMPs (after EPA-SUSTAIN and BLIP), runoff at the outlet is 177.22 mm, showing a reduction of 21.54 mm. 495,607 BMPs occupying 76.99 km^2 are facilitated for this purpose. Similarly, for RCPs 6.0 and 8.5, extreme rainfalls are 440.35 and 624.2 mm, and consequently, the runoff produced is 428.35 and 602.65 mm. Runoff after placement of 492,149 and 492,916 BMPs (occupying 76.73 and 77.09 km^2) in RCPs 6.0 and 8.5 is 389.63 and 547.62 mm, respectively, for the situation of 100% BA and 3.05% (for RCP 6.0) and 3.09% (for RCP 8.5) pollutant load reduction. Corresponding runoff reduced due to these BMPs is 38.72 and 55.03 mm and water saved in this process could meet the water demands of GHMC for 10.33 and 11.53 days.

The research work presented in this paper is helpful to society as maximum runoff reduction and pollutant load reduction are needed. Runoff captured by implementing BMPs will help satisfy the drinking water requirements of the community though partially. In addition, pollutant reduction can minimize health hazards in this process. We believe that this simultaneous management of both quality and quantity of water and related further research undoubtedly improve quality of life. Another potential of the work is its interdisciplinary nature where researchers from chemistry, social sciences, and biology can also participate. In addition, potential areas researchers can explore are sizing of BMPs, potable water efficiency, considering many other pollutants and future land availability projections into the existing modeling framework.

Keeping in view the advantages of BMP placement, an immediate action plan can be implemented for betterment of Hyderabad. Rainwater harvesting structures in a building can be made a mandatory requirement while planning the construction of buildings. It can be followed by using available open spaces. We also hope it will help the policymakers in reliable and easy decision-making.

ACKNOWLEDGEMENTS

This work is supported by Information Technology Research Academy (ITRA), Government of India under ITRA-water grant ITRA/15(68)/water/IUFM/01. The third author would like to acknowledge the funding support provided by the Council of Scientific and Industrial Research (CSIR), New Delhi, through a project with reference number 22(0782)/19/EMR-II dated 24.7.19. Special acknowledgments go to Prof D. Nagesh Kumar, Indian Institute of Science, Bangalore, for providing valuable guidance during the revision of the manuscript and critical suggestions. We also thank the editor and two anonymous reviewers for their valuable inputs. The authors thank GHMC officials and other agencies for providing all the support.

CONFLICT OF INTEREST

The authors declare that they have no conflict of interests.

DATA AVAILABILITY STATEMENT

Data cannot be made publicly available; readers should contact the corresponding author for details.

REFERENCES

Adham, A., Riksen, M., Ouessar, M. & Ritsema, C. J. 2016 A methodology to assess and evaluate rainwater harvesting techniques in (semi-) arid regions. *Water* **8** (5), 198.

Antolini, F., Tate, E., Dalzell, B., Young, N., Johnson, K. & Hawthorne, P. L. 2020 Flood risk reduction from agricultural best management practices. *JAWRA Journal of the American Water Resources Association* **56** (1), 161–179.

Avashia, V. & Garg, A. 2020 Implications of land use transitions and climate change on local flooding in urban areas: an assessment of 42 Indian cities. *Land Use Policy* **95**, 104571.

Battiata, J., Collins, K., Hirschman, D. & Hoffmann, G. 2010 The runoff reduction method. *Journal of Contemporary Water Research & Education* **146** (1), 11–21.

Beck, A. 2014 *Evaluating Best Management Practices Scenarios in Ballona Creek Watershed Using EPA's SUSTAIN Model*. Master's Thesis, Faculty and the Board of Trustees, Colorado School of Mines.

Boguniewicz-Zabłocka, J. & Capodaglio, A. G. 2020 Analysis of alternatives for sustainable stormwater management in small developments of polish urban catchments. *Sustainability* **12** (23), 10189.

Braune, M. J. & Wood, A. 1999 Best management practices applied to urban runoff quantity and quality control. *Water Science and Technology* **39** (12), 117–121.

Cheng, M. S., Zhen, J. X. & Shoemaker, L. 2009 BMP decision support system for evaluating storm-water management alternatives. *Frontiers of Environmental Science & Engineering in China* **3** (4), 453–463.

CPHEEO Manual 1999 *Manual on Water Supply and Treatment*. Available from: http://cpheeo.gov.in/cms/manual-on-water-supply-and-treatment.php (accessed 4 April 2020).

Das, J., Treesa, A. & Umamahesh, N. V. 2018 Modelling impacts of climate change on a river basin: analysis of uncertainty using REA & possibilistic approach. *Water Resources Management* **32** (15), 4833–4852.

EPA-SUSTAIN 2014 *System for Urban Stormwater Treatment and Analysis INtegration (SUSTAIN) Tool for Selecting Best Management Practices to Protect Water Quality*. Available from: https://www.epa.gov/water-research/system-urban-stormwater-treatment-and-analysis-integration-sustain (accessed 4 April 2020).

Esmail, B. A. & Suleiman, L. 2020 Analyzing evidence of sustainable urban water management systems: a review through the lenses of sociotechnical transitions. *Sustainability* **12** (11), 4481.

GHMC 2011a *Delimitation of Election Wards*. Available from: https://web.archive.org/web/20111110083915/http://www.ghmc.gov.in/tender%20pdfs/election_wards.pdf (accessed 4 April 2020).

GHMC Population 2011b *Population of Hyderabad*. Available from: http://www.populationu.com/cities/hyderabad-population (accessed 9 October 2020).

Google Earth v 6 2016 Hyderabad, Telangana, India, 17.45 lat, 78.44 long at eye alt 35.16 miles (accessed May 2016).

Gülbaz, S. & Kazezyilmaz-Alhan, C. M. 2015 Investigating the effects of low impact development (LID) on surface runoff and TSS in a calibrated hydrodynamic model. *Journal of Urban and Environmental Engineering* **9** (2), 91–96.

HMDA 2019 *Master Plan of the City*. Available from: hmdaprojects.hmda.gov.in/masterplan. (accessed September 2019).

HMWSSB 2012 *Hydrate Hyderabad*. Available from: https://jalamjeevam.telangana.gov.in/about-hyderabad/about-jalam-jeevam/ (accessed 4 April 2020).

HMWSSB 2018 *Telangana Rainwater Harvesting Portal*. Available from: https://telangana.gov.in/news/2018/06/rain-water-harvesting (accessed 20 December 2018).

Hou, J., Liu, F., Tong, Y., Guo, K., Ma, L. & Li, D. 2020 Numerical simulation for runoff regulation in rain garden using 2D hydrodynamic model. *Ecological Engineering* **153**, 105794.

HSLDA 2016 *Water Level Information of Hussain Sagar Lake*. Unpublished Report.

Islam, A., Shirsath, P. B., Kumar, S. N., Subash, N., Sikka, A. K. & Aggarwal, P. K. 2014 Modeling water management and food security in India under climate change. In: *Practical Applications of Agricultural System Models to Optimize the Use of Limited Water* (L. R. Ahuja, L. Ma & R. J. Lascano, eds.), Vol. 5, John Wiley & Sons, Madison, WI, pp. 267–315.

Javadinejad, S., Dara, R. & Jafary, F. 2021 Climate change simulation and impacts on extreme events of rainfall and storm water in the Zayandeh Rud Catchment. *Resources Environment and Information Engineering* **3** (1), 100–110.

Jia, H., Yao, H., Tang, Y., Shaw, L. Y., Field, R. & Tafuri, A. N. 2015 LID-BMPs planning for urban runoff control and the case study in China. *Journal of Environmental Management* **149**, 65–76.

Karunanidhi, D., Anand, B., Subramani, T. & Srinivasamoorthy, K. 2020 Rainfall-surface runoff estimation for the Lower Bhavani basin in south India using SCS-CN model and geospatial techniques. *Environmental Earth Sciences* **79** (13), 1–19.

Khaing, M. 2015 Assessing climate change impacts on hydropower generation in the Myitnge river basin, Myanmar. *Hydropower's 15*, Norway.

Kuntiyawichai, K., Sri-Amporn, W., Wongsasri, S. & Chindaprasirt, P. 2020 Anticipating of potential climate and land use change impacts on floods: a case study of the lower Nam Phong River Basin. *Water* **12** (4), 1158.

Kurkalova, L. A. 2014 *On Optimal Placement of Best Management Practices in Agricultural Watersheds (No. 329-2016-13285)*.

Lee, J. G., Selvakumar, A., Alvi, K., Riverson, J., Zhen, J. X., Shoemaker, L. & Lai, F. H. 2012 A watershed-scale design optimization model for storm-water best management practices. *Environmental Modelling & Software* **37**, 6–18.

Lee, J. Y., Son, H. J., Kim, D., Ryu, J. H. & Kim, T. W. 2021 Evaluating the hydrologic risk of n-year floods according to RCP scenarios. *Water* **13** (13), 1805.

Lewellyn, C., Lyons, C. E., Traver, R. G. & Wadzuk, B. M. 2016 Evaluation of seasonal and large storm runoff volume capture of an infiltration Green infrastructure system. *Journal of Hydrologic Engineering* **21** (1), 04015047.

Li, F., Yan, X. F. & Duan, H. F. 2019 Sustainable design of urban storm-water drainage systems by implementing detention tank and LID measures for flooding risk control and water quality management. *Water Resources Management* **33** (9), 3271–3288.

Loáiciga, H. A., Sadeghi, K. M., Shivers, S. & Kharaghani, S. 2015 Storm-water control measures: optimization methods for sizing and selection. *Journal of Water Resources Planning and Management* **141** (9), 04015006.

Lompi, M., Mediero, L. & Caporali, E. 2021 Future flood hazard assessment for the City of Pamplona (Spain) using an ensemble of climate change projections. *Water* **13** (6), 792.

Lucas, W. C. & Sample, D. J. 2015 Reducing combined sewer overflows by using outlet controls for Green Stormwater Infrastructure: case study in Richmond, Virginia. *Journal of Hydrology* **520**, 473–488.

Malik, A. & Kumar, A. 2020 Spatio-temporal trend analysis of rainfall using parametric and non-parametric tests: case study in Uttarakhand, India. *Theoretical and Applied Climatology* **140** (1), 183–207.

Mandal, U., Sena, D. R., Dhar, A., Panda, S. N., Adhikary, P. P. & Mishra, P. K. 2021 Assessment of climate change and its impact on hydrological regimes and biomass yield of a tropical river basin. *Ecological Indicators* **126**, 107646.

Nayan, N. K., Das, A., Mukerji, A., Mazumder, T. & Bera, S. 2020 Spatio-temporal dynamics of water resources of Hyderabad Metropolitan Area and its relationship with urbanization. *Land Use Policy* **99**, 105010.

Nilawar, A. P. & Waikar, M. L. 2019 Impacts of climate change on streamflow and sediment concentration under RCP 4.5 and 8.5: a case study in Purna river basin, India. *Science of the Total Environment* **650**, 2685–2696.

Oleyiblo, J. O. & Li, Z. J. 2010 Application of HEC-HMS for flood forecasting in Misai and Wan'an catchments in China. *Water Science and Engineering* **3** (1), 14–22.

Open Street Maps(OSM) 2016. https://download.geofabrik.de/asia/india.html (accessed July 2017).

Pournara, C. 2013 Teachers' knowledge for teaching compound interest. *Pythagoras* **34** (2), 1–10.

Qin, H. P., Li, Z. X. & Fu, G. 2013 The effects of low impact development on urban flooding under different rainfall characteristics. *Journal of Environmental Management* **129**, 577–585.

Ramachandran, A., Palanivelu, K., Mudgal, B. V., Jeganathan, A., Guganesh, S., Abinaya, B. & Elangovan, A. 2019 Climate change impact on fluvial flooding in the Indian sub-basin: a case study on the Adyar sub-basin. *PLoS ONE* **14** (5), e0216461.

Ramly, S. & Tahir, W. 2016 Application of HEC-GeoHMS and HEC-HMS as rainfall–runoff model for flood simulation. In: *ISFRAM 2015*. Springer, Singapore, pp. 181–192.

Rangari, V. A., Umamahesh, N. V. & Patel, A. K. 2021 Flood-hazard risk classification and mapping for urban catchment under different climate change scenarios: a case study of Hyderabad city. *Urban Climate* **36**, 100793.

Rao, V. G. & Surinaidu, L. 2012 Rain gardens – a new ecosystem in city landscape for in situ harvesting of rain water. *Memoirs of the Geological Survey of India* **80**, 89–96.

Ridwan, W. M., Sapitang, M., Aziz, A., Kushiar, K. F., Ahmed, A. N. & El-Shafie, A. 2021 Rainfall forecasting model using machine learning methods: case study Terengganu, Malaysia. *Ain Shams Engineering Journal* **12** (2), 1651–1663.

Rukundo, E. & Doğan, A. 2016 Assessment of climate and land use change projections and their impacts on flooding. *Polish Journal of Environmental Studies* **25** (6), 2541–2551.

Sadeghi, K. M., Loáiciga, H. A. & Kharaghani, S. 2018 Storm-water control measures for runoff and water quality management in urban landscapes. *JAWRA Journal of the American Water Resources Association* **54** (1), 124–133.

Sannigrahi, S., Bhatt, S., Rahmat, S., Uniyal, B., Banerjee, S., Chakraborti, S. & Bhatt, A. 2018 Analyzing the role of biophysical compositions in minimizing urban land surface temperature and urban heating. *Urban Climate* **24**, 803–819.

Sarma, J. & Rajkhowa, S. 2021 Urban floods and mitigation by applying ecological and ecosystem engineering. In: *Handbook of Ecological and Ecosystem Engineering* (M. N. V. Prasad, ed.), John Wiley & Sons, Hoboken, NJ, pp. 201–218.

Sarminingsih, A., Rezagama, A. & Ridwan 2019 Simulation of rainfall-runoff process using HEC-HMS model for Garang Watershed, Semarang, Indonesia. *Journal of Physics: Conference Series* **1217** (1), 012134.

Shishegar, S., Duchesne, S. & Pelletier, G. 2018 Optimization methods applied to storm-water management problems: a review. *Urban Water Journal* **15** (3), 276–286.

Sun, Y., Tong, S. & Yang, Y. J. 2016 Modeling the cost-effectiveness of storm-water best management practices in an urban watershed in Las Vegas Valley. *Applied Geography* **76**, 49–61.

Surwase, T. & Manjusree, P. 2019 Urban flood simulation - a case study of Hyderabad city. In: *National Conference on Flood Early Warning for Disaster Risk Reduction*, 30–31 May 2019, Hyderabad, pp. 133–143.

Swathi, V. 2020 *Analysing the Linkages Between Urban Floods, Climate Change and Land Use*. PhD Thesis, BITS Pilani Hyderabad Campus.

Swathi, V., Srinivasa Raju, K. & Sai Veena, S. 2020 Modelling impact of future climate and land use land cover on flood vulnerability for policy support – Hyderabad, India. *Water Policy* **22** (5), 733–747.

Taylor, K. E., Stouffer, R. J. & Meehl, G. A. 2012 An overview of CMIP5 and the experiment design. *Bulletin of the American Meteorological Society* **93** (4), 485–498.

The Times of India 2018 *Ailing and Dirty, Lakes in Hyderabad Present Dismal Report Card*. Available from: https://m.timesofindia.com/city/hyderabad/ailing-and-dirty-lakes-in-hyderabad-present-dismal-report-card/amp_articleshow/66116298.cms

USACE 2009 *HEC-GeoHMS Geospatial Hydrologic Modeling Extension: User's Manual*. U.S Army Corps of Engineers, Washington, DC, p. 197.

USGS 2016 *ASTER Data*. Available from: http://earthexplorer.usgs.gov/ (accessed January 2016).

Vemula, S., Raju, K. S., Veena, S. S. & Kumar, A. S. 2019 Urban floods in Hyderabad, India, under present and future rainfall scenarios: a case study. *Natural Hazards* **95** (3), 637–655.

Warganda, T. K. & Sutjiningsih, D. 2017 Placement of BMPs in urban catchment area using SUSTAIN model: case study at Universitas Indonesia Campus, Depok, West Java, Indonesia. In: *MATEC Web of Conferences*, Vol. 138. EDP Sciences, p. 06007.

Wu, J., Chen, Y., Yang, R. & Zhao, Y. 2020 Exploring the optimal cost-benefit solution for a low impact development layout by Zoning, as well as considering the inundation duration and inundation depth. *Sustainability* **12** (12), 4990.

Yao, L., Chen, L., Wei, W. & Sun, R. 2015 Potential reduction in urban runoff by green spaces in Beijing: a scenario analysis. *Urban Forestry & Urban Greening* **14** (2), 300–308.

You, L., Xu, T., Mao, X. & Jia, H. 2019 Site-scale LID-BMPs planning and optimization in residential areas. *Journal of Sustainable Water in the Built Environment* **5** (1), 05018004.

Zhou, Q., Leng, G. & Huang, M. 2018 Impacts of future climate change on urban flood volumes in Hohhot in northern China: benefits of climate change mitigation and adaptations. *Hydrology and Earth System Sciences* **22** (1), 305–316.

Zhou, Q., Leng, G., Su, J. & Ren, Y. 2019 Comparison of urbanization and climate change impacts on urban flood volumes: importance of urban planning and drainage adaptation. *Science of the Total Environment* **658**, 24–33.

Zhuang, M., Lu, X., Caro, D., Gao, J., Zhang, J., Cullen, B. & Li, Q. 2019 Emissions of non-CO_2 greenhouse gases from livestock in China during 2000–2015: magnitude, trends and spatiotemporal patterns. *Journal of Environmental Management* **242**, 40–45.

Zoppou, C. 2001 Review of urban storm water models. *Environmental Modelling & Software* **16** (3), 195–231.

First received 17 August 2021; accepted in revised form 2 December 2021. Available online 21 December 2021